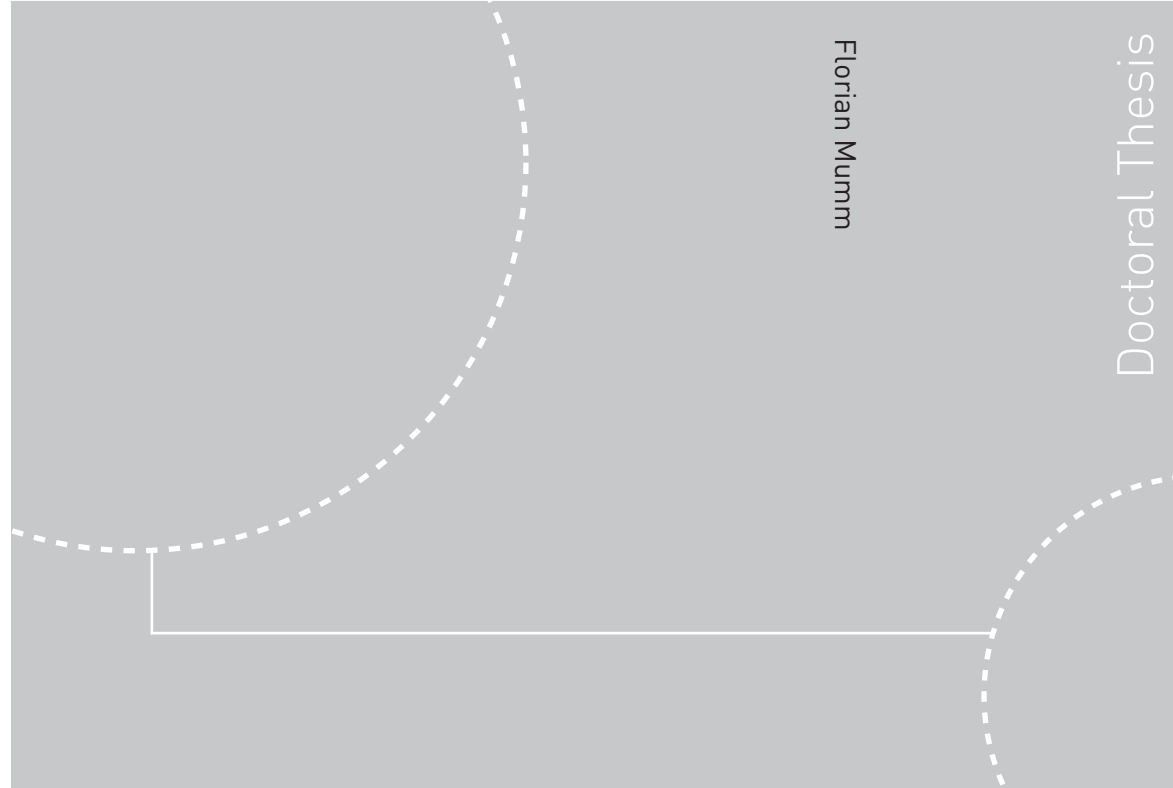



ISBN 978-82-471-2483-3 (printed ver.)
ISBN 978-82-471-2485-7 (electronic ver.)
ISSN 1503-8181




Florian Mumm

Doctoral Thesis

Doctoral theses at NTNU,  ;

Florian Mumm
**Interactions of High Aspect Ratio
Nanostructures and Biological
Systems**

Doctoral theses at NTNU, 2010:245 

NTNU
Norwegian University of
Science and Technology
Thesis for the degree of
philosophiae doctor
Faculty of Natural Sciences and Technology
Department of Physics

 **NTNU**
Norwegian University of
Science and Technology

 **NTNU**

 **NTNU**
Norwegian University of
Science and Technology

Florian Mumm

Interactions of High Aspect Ratio Nanostructures and Biological Systems

Thesis for the degree of philosophiae doctor

Trondheim, December 2010

Norwegian University of
Science and Technology
Faculty of Natural Sciences and Technology
Department of Physics



Norwegian University of
Science and Technology

NTNU

Norwegian University of Science and Technology

Thesis for the degree of philosophiae doctor

Faculty of Natural Sciences and Technology
Department of Physics

©Florian Mumm

ISBN 978-82-471-2483-3 (printed ver.)

ISBN 978-82-471-2485-7 (electronic ver.)

ISSN 1503-8181

Doctoral Theses at NTNU, 2010:245

Printed by Tapir Uttrykk

Acknowledgements

First of all I would like to thank my supervisor associate professor Pawel Sikorski for his constant interest in what I was doing, for all the constructive feedback, as well as for the freedom I enjoyed throughout my thesis – and for at least a thousand motivating “How’s it going?” questions over the years.

I would also like to thank professor Markku Leskelä and lecturer Marianna Kemell for the nice and hopefully expanding cooperation we had and for giving me (even more) good reasons to visit Helsinki twice.

Furthermore, I would like to thank the members of the Biophysics group at NTNU for creating such a positive atmosphere both inside the lab and on our various activities in and around of Trondheim, in particular Sven for the time, when we shared an office, Kata for the interesting discussions and for granting me “asylum” at the AFM when incubations took time, and Sylvie for all the cakes and for tirelessly organising so many activities of the group.

I would also like to thank my cooperators at NTNU, researcher Sabina Strand for her help with biotechnology and associate professor Ton van Helvoort for conducting the TEM experiments and for spreading his enthusiasm for physics and nanotechnology.

Finally I would like to thank my friends and family for their support and for making the last few years such a remarkable time.

This work has been carried out at the Department of Physics at The Norwegian University of Science and Technology from 2006 to 2010 with financial support from NTNU Nanolab.

Summary

As the length scale of basic biological processes coincides more and more with the length scale at which artificial nanostructures can be constructed, the interplay between those structures and biological systems becomes an increasingly promising field of research. This thesis is centred around high aspect ratio inorganic nanostructures, such as nanotubes and nanowires and how they can be made using biological structures, as well as how they can be used to manipulate biological systems.

Two different approaches were taken: First, the very regular nanoporous structure, which makes up the spines of the bristle worm *Aphrodita Aculeata* (sea mouse) was used as a template to produce nanowires and nanotubes with a diameter of about 200 nm and a length of a few hundred microns. Nanowires made of nickel and copper were produced by electrodeposition and nanotubes made of aluminium oxide were produced by atomic layer deposition. Additionally, it was shown that the sea mouse spine based template was rigid enough to withstand a wide range of pH and temperatures, which should make it possible to grow nanostructures of a variety of materials by adopting fabrication procedures developed for membrane based nanoporous templates.

In a second approach, vertically aligned arrays of copper oxide nanowires were grown in a catalyst-free thermal oxidation process on copper substrates. Methods of patterning were developed for the substrates and their nanowire decoration as well as a method for growing wires in large homogeneous arrays on inexpensive copper foils. Patterned copper substrates with and without a coating of nanowires were then used as the basis for a superhydrophobic droplet microfluidic system.

Finally, the homogeneous arrays of vertically aligned copper oxide nanowires were integrated into photoresist microstructures made by traditional UV lithography to construct a transparent, cell friendly, compartmentalised system, which is intended to serve as a platform to transfect cells by impalement.

Contents

1	Introduction to the thesis	7
2	Concepts	9
2.1	Nanotube and nanowire fabrication	9
2.1.1	Template based nanostructure fabrication . . .	9
2.1.2	Template free nanostructure fabrication	14
2.2	Self assembled (mono-)layers	16
2.3	Superhydrophobic surfaces	18
2.4	Digital microfluidics	20
2.5	Nanostructure cell-impalement	20
3	Summary of the papers	22
3.1	Paper I	22
3.2	Paper II	22
3.3	Paper III	23
3.4	Paper IV	23
4	General discussion	24
4.1	The sea mouse based nanoporous template	24
4.2	Interaction of CuO nanowires and biological systems .	25
5	Conclusions and Outlook	28
6	Paper I	36
7	Paper II	45
8	Paper III	59
9	Paper IV	72

List of papers

Paper I

F. Mumm, M. Kemell, M. Leskelä, and P. Sikorski:

A bio-originated porous template for the fabrication of very long, inorganic nanotubes and nanowires. Bioinspiration & Biomimetics, 5, 026005, 2010.

Paper II

F. Mumm and P. Sikorski:

Oxidative Fabrication of Patterned, Large, Defect-Free CuO Nanowire arrays. Submitted to Nanotechnology.

Paper III

F. Mumm, T. van Helvoort, and P. Sikorski:

An Easy Route to Superhydrophobic Copper based Droplet Microfluidic Chips. ACS nano, 3 (9), 2647, 2009.

Paper IV

F. Mumm, K. Beckwith, S. Strand, S. Lelu, and P. Sikorski

An epoxy/copper oxide nanowire based cell impalement system. In preparation.

Contribution to the papers

Most of the papers are based on projects, which involved the cooperation with other scientists. Their contribution to the experimental work is given below. All the other experiments as well as the writing of the publications included in the thesis was carried out by me.

Paper I: Atomic layer deposition was carried out by Marianna Kemell and Markku Leskelä at the Department of Chemistry, University of Helsinki.

Paper III: TEM imaging, EDS, and EELS was done by Ton van Helvoort, Department of Physics, NTNU.

Paper IV: Some devices made by the integration of nanowire-covered SU-8 membranes in larger microstructures were made by Kai Beckwith, Department of Physics, NTNU. Planing and preparations for some cell culturing experiments were carried out by Sabina Strand, Department of Biotechnology, NTNU and Sylvie Lelu, Department of Physics, NTNU.

1 Introduction to the thesis

The work presented in this thesis is centred around the interplay of high aspect ratio nanostructures such as nanotubes and nanowires and biological systems. The work was done from 2006 to 2010 in the biophysics group at NTNU. In the course of the thesis, two different perspectives were taken:

In the first part, a method was developed to use well defined biological structures as templates for the fabrication of nanotubes and nanowires. This approach represents the “from the biological world to nanofabrication” view of bionanotechnology. It aims to combine nature’s ability to precisely manufacture nanoscale structures with traditional nanofabrication procedures. This can be either done by integrating bio-originated structures directly, or by utilising the processes, which make them.

Examples of the “from biology to nanofabrication” approach include the controlled self assembly of biological units to form larger scale structures like peptide nanotubes¹ or almost arbitrary shapes made of DNA (DNA origami^{2,3}), the fabrication of nanoscale objects within bio-originated moulds, as shown for nanowires made in peptide⁴ and lipid⁵ nanotubes and even in viruses⁶.

Finally functional biological units can be integrated in larger devices as e.g. demonstrated for α -hemolysin nanopores in a lipid bilayer, which could be used to discriminate between different nucleotides⁷ or a nanoscale propeller consisting of a biomolecular motor (the rotary part of an ATP synthase) and an inorganic rotor blade (a nickel nanowire)⁸.

In the second part of the thesis, vertically aligned arrays of inorganic nanowires were interfaced with biological systems. This approach represents the “from nanofabrication to the biological world” view of bionanotechnology, which aims to use artificial nanostructured devices to probe or control biological processes.

Examples of this include minituarised devices like nanowire based biosensors^{9,10} or nanofluidic DNA analysis tools^{11,12} which aim to replace present day larger scale systems as well as devices exploiting new phenomena happening at the nanoscale. Such phenomena include the gentle cell penetration by nanowires¹³, which can be used in reverse

transfection methods^{14,15} or to introduce electrodes¹⁶.

Especially the approach to apply micro and nanofabricated tools and devices to study biological systems has in recent years developed into an exciting field of research as the length scales, which are achievable in nanofabrication and those on which fundamental biological processes take place more and more coincide.

Of the research presented in this thesis, the first paper represents the “from biology to nanofabrication” approach, where a biooriginated structure was used as a fabrication tool to produce inorganic nanotubes and nanowires, whereas the other papers represent the “from nanofabrication to biology” approach, where nanostructures made by more traditional methods were used to interact with biological systems.

Despite the complementary perspectives, many characterization and fabrication procedures, such as electrodeposition and etching, as well as a variety of thermal processes and microscopy techniques, could be applied in several publications.

2 Concepts

A variety of different fabrication and application concepts have been used in this thesis. The following section briefly presents the most central ones with special attention to the actual implementations used in the publications. First, fabrication methods are explained followed by some background on the fields, to which the fabricated structures were applied.

2.1 Nanotube and nanowire fabrication

Nanotubes and nanowires can be produced using a variety of different methods, which can be divided in bottom-up (controlled assembly of required compounds) and top-down (controlled removal of not-required compounds) approaches. This thesis exclusively deals with bottom-up produced nanostructures, fabricated using both template based as well as template free systems.

2.1.1 Template based nanostructure fabrication

Whereas template-free methods usually require specific fabrication procedures for nanostructures made of different materials, template based methods are often more generally applicable once a suitable template is available. Of the variety of templates introduced so far, porous anodic alumina and track-etched polycarbonate membranes are most commonly used¹⁷. The shape, length, and diameter of the nanostructures produced in these membranes is given by the diameter and profile of the individual nanopores and the membranes thickness. For some materials unconventional templates like controlled surface cracks¹⁸ or layered substrates for step edge decoration¹⁹ have been developed to overcome the length restriction imposed by the limited thickness of the membranes. Paper I presents a new type of such unconventional templates, which is based on a biological nanostructure.

Below, an introduction is given to nanofabrication using templates from nature, as well as a short description of electrodeposition and atomic layer deposition as the two fabrication methods, which were used in this thesis.

Nanofabrication using biological templates

The precise assembly of nanometre sized objects is a task routinely accomplished by nature as all biological structures are assembled in a bottom up fashion from nanoscale building blocks such as proteins, lipids, or polysaccharides as well as through size controlled biomineralisation. During the course of evolution, biological compounds have been optimized for a variety of properties, depending on their function in the organism. Often these functions originate specifically from the compound's micro and nanostructure assembly. In the transfer to man made technology, such assemblies can serve either as direct moulds in the aim to replicate their function or as sources of inspiration for the fabrication of new materials^{20,21}.

One main focus in the direct use of biooriginated nanostructures to copy their function is placed on the replication of optically active topologies as they are easy to harvest and offer a variety of potential technological applications. Using atomic layer deposition, it could e.g. been shown, that both the very low reflectivity of a fly's eye²² as well as the characteristic reflection spectrum of butterfly wings²² are inherited by Al₂O₃ replicas of their respective nanostructures.

Additionally, biooriginated structures can be employed for uses different from their original function. This is e.g. the case for the fabrication of nanowires in the central channel of the tobacco mosaic virus⁶ or along different fibrous structures such as actin filaments or DNA strands²³. Paper I follows this approach and utilizes a biooriginated array of parallel nanochannels originally composing a photonic crystal²⁴ as a mould to produce nanowires and nanotubes by electro-deposition and atomic layer deposition.

Electrodeposition

Electrodeposition (or electroplating) is based on the deposition of a solid material at the surface of an electrode, which is immersed in an electrolyte. To use it as a method for making nanowires, the electrode is deposited at the backside of a porous template in such a way that it is only accessible through the pores. Connected to such a template, nanowires made of conductive (or semiconductive) materials grow from the electrode along the pores through the template.

In this thesis, electrodeposition is conducted in an electrolytic cell

with two metal electrodes (made of Cu or Ni) and an electrolyte containing the respective metal ions. The necessary potential to drive the deposition was provided by a standard laboratory power source. Besides nanowire fabrication, electrodeposition was also used to produce macroscopic structures. The working electrode, i.e. the electrode onto which the material is deposited was either a gold layer, sputter coated at the backside of the nanoporous template, (paper I, illustrated in Figure 1) or a copper substrate (papers II and III). In paper II, certain areas of the copper foil are excluded from the deposition process by shielding them from the electrolyte using ink or laser printer toner.

The used electrolytes were all aqueous solutions of salts containing the material to be deposited, namely CuSO_4 , NiSO_4 , and NiCl_2 . In all cases, the cell potential E_{cell} was zero as is evident from the Nernst equation:

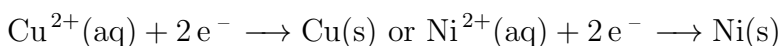
$$E_{cell} = E_{cell}^{\ominus} - \frac{RT}{zF} \ln \frac{a_{electrode1}}{a_{electrode2}}$$

E_{cell}^{\ominus} is the standard cell potential of the used electrochemical cell, which was always zero as the same reaction (in reverse direction) took place at both electrodes (illustrated for Cu deposition in Figure 1). R is the universal gas constant, T the temperature, F the Faraday constant, and z is the number of transferred electrons. As both electrodes share the same electrolyte, the fraction of the two activities $a_{electrode1}$ and $a_{electrode2}$ at the two electrodes is one, which results in a logarithm of zero and a total cell potential of 0 V.

The actual potential applied in the experiments to drive the deposition, was adopted from previously published procedures^{25,26,27}, which have shown to be suitable for the deposition of copper or nickel.

Under the applied potential, the positively charged metal ions deposited at the negatively charged working electrode. A wire made of either copper or nickel served as a sacrificial counter electrode, to supply new ions to the electrolyte. The reactions happening separately at the cathode and the anode are given below²⁸ (see also Figure 1):

At the cathode:



At the anode:

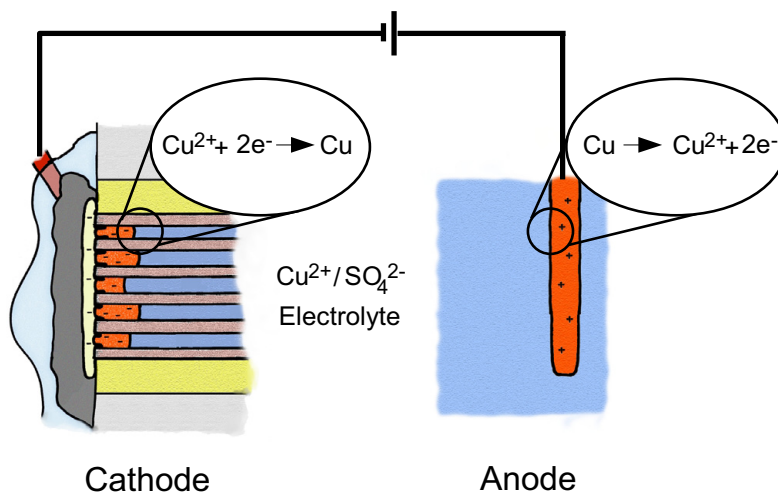
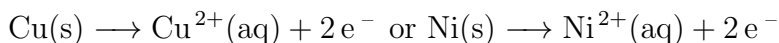


Figure 1: Sketch of nanowire growth and electrode reactions for the electrodeposition of Cu nanowires in a template

A special case is the electrodeposition under hydrogen evolution used in paper III. Here, at high potentials, the deposition of copper at the cathode competes with other processes such as hydrogen evolution from the electrolysis of water²⁷ and the evolving hydrogen bubbles served as temporary templates for the fabrication of porous copper structures around them. For this experiment a graphite rod was used as the counter electrode as copper wires rapidly passivated.

Atomic layer deposition

Atomic layer deposition (ALD) is a self limiting, vapour phase, layer by layer deposition technique²⁹ used in paper I (as well as potentially

used with the system presented in paper IV). Thin films are deposited by sequential deposition of atomic layers from their respective precursors. ALD can be used to produce very controlled nanotubes by thin film deposition at the walls of a nanoporous template as in paper I or on the outside of vertical nanowires as potentially used in paper IV. After the deposition, the template is dissolved. A typical deposition cycle for the production of Al_2O_3 nanotubes starts with a purging step using inert N_2 followed by a first deposition step using $\text{Al}(\text{CH}_3)_3$ (Trimethylaluminium, TMA) of which one methyl group reacts with a hydroxyl group at the surface to form an O - Al bond and methane. The methane is removed in a subsequent purging step with N_2 and gas phase water is inserted as the second reaction precursor. The water reacts with the remaining methyl groups resulting in the formation of new hydroxyl groups, Al-O-Al bonds, and methane gas³⁰, see Figure 2. Afterwards the cycle can start again with a new reaction of TMA.

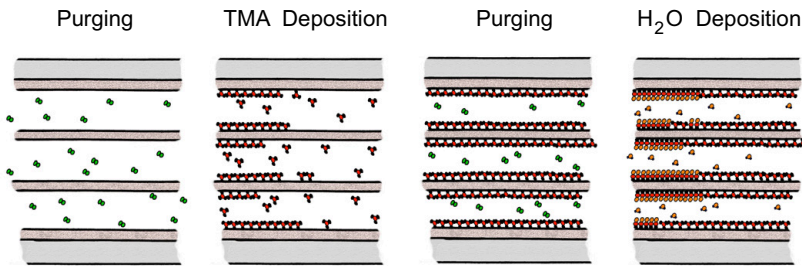


Figure 2: Illustration of one ALD deposition cycle for the production of Al_2O_3 nanotubes in a template

As film growth can only take place at surface sites made available by the previous precursor, deposition automatically ends once all the reactive groups are consumed. This self limitation makes ALD especially suitable for coatings within high aspect ratio structures, as spatial differences in the concentration of the initial precursors do not lead to inhomogeneous film growth.

2.1.2 Template free nanostructure fabrication

Template free nanotubes and nanowires are grown by promoting the crystallization of solids along one direction³¹. The most commonly used approaches are vapour based systems, notably the vapour-liquid-solid mechanism, where precursors of the nanostructures are supplied as gas phase reactants and growth occurs at the interface between a liquid droplet of a catalyst metal and the solid support or the growing nanostructure³¹. Additionally, solution based methods like template free electrodeposition³² or selective growth using capping agents³³ have been presented.

The CuO nanowires used in this thesis are produced via a catalyst-free thermal oxidation method³⁴. Oxidative growth of metal oxide nanowires is a simple and inexpensive technique based on heating of the respective metal substrates in an oxygen rich atmosphere. Apart from CuO, such growth procedures have been presented for a variety of materials such as Fe₂O₃³⁵, Co₃O₄³⁶, ZnO³⁷, or V₂O₅³⁸.

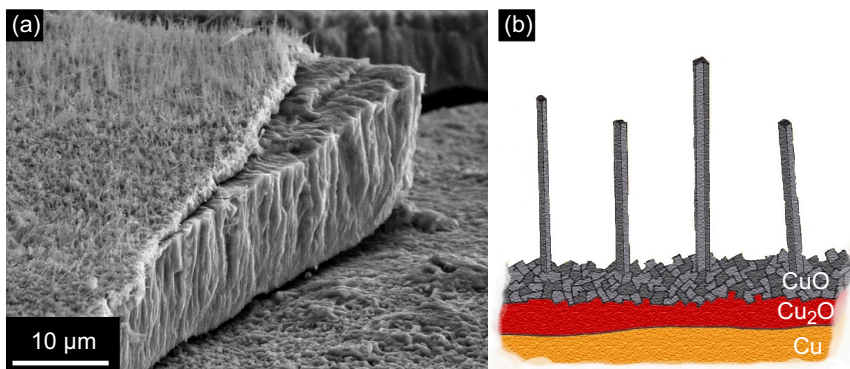


Figure 3: CuO nanowires formed on a Cu substrate. (a): SEM image of the Cu/Cu₂O/CuO layers, (b): Sketch of the surface composition

After the oxidation, the CuO nanowires form the top part of a Cu/Cu₂O/CuO layer system³⁴ as shown in Figure 3. The nanowires grow directly from the Cu₂O layer. It has been shown that all three

layers are necessary to obtain dense nanowire arrays³⁹.

The growth mechanism underlying the formation of CuO nanowires by thermal oxidation is still under debate. Presented models attribute nanowire formation to a vapour-solid growth process⁴⁰, to stress relaxation at the Cu₂O/CuO interface⁴¹, or to competing grain boundary and lattice diffusion of copper ions across the Cu₂O layer^{42,43}.

The vapour-solid based growth mechanism, which was originally proposed mostly because a vapour-liquid-solid mechanism was excluded, is now generally rejected based on the low process temperature in relation to the melting points of the involved materials and their correspondingly low vapour pressure^{43,44}.

In contrast to vapour-solid (and vapour-liquid-solid) based growth models, where new material is added on the top of the growing nanostructures, both alternative models for the formation of CuO nanowires attribute their growth to new material being supplied at the bottom (leaving it open if that material is subsequently transported up the wire).

The presentation of the stress relaxation model⁴¹ is somewhat inconsistent, as the model includes a saturation of the length of the wires with increasing annealing time attributed to all stress being released, whereas the experimental part of the paper states that the wire length increases with time and no saturation was observed.

In contrast, the models based on competing diffusion processes of copper across the Cu₂O layer fits well to experimental results^{42,43}. According to this model, nanowire growth is based on grain boundary-diffusion of Cu ions through the Cu₂O layer and oxygen ions through the CuO layer as illustrated in Figure 4 (c).

Consequently, growth occurs in a temperature window, where Cu ions are mobile enough to get through the oxide layer. The lower limit is set to about 400° due to decreased thermal motion, whereas the upper limit at roughly 700° is based on the replacement of the relatively fast grain-boundary diffusion by slower lattice diffusion⁴³. A similar model has been proposed for the growth of Fe₂O₃ nanowires⁴⁵.

Recently, the influence of the electric field created by the ionization of oxygen adsorbed at the CuO/air interface and copper in the substrate (resulting in the O²⁻ and Cu²⁺ ions) in diffusion based models has been discussed. Its relevance could be shown by demonstrating

that an external electric field present during nanowire growth can be used to control their length⁴⁴.

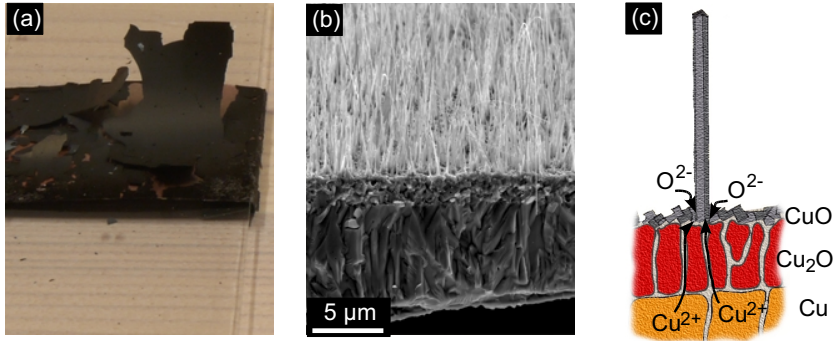


Figure 4: Thermally grown CuO Nanowires: (a): Oxidised surface showing flaking (b): Details of the detached oxide layers (c): Growth model adopted from⁴³.

A problem in applications of thermally grown CuO nanowire arrays is the large surface mismatch between copper and Cu₂O. When the sample is cooled down after nanowire fabrication, this commonly leads to the oxide layers detaching from the Cu substrate^{46,47} as shown in 4 (a) and (b). Paper II presents a setup, showing how this flaking can be prevented.

2.2 Self assembled (mono-)layers

Self-assembled monolayers (SAMs) are frequently used as a simple way to modify the surface properties of metals, metal oxides, and semiconductors⁴⁸. As nanostructures most often offer a high surface area compared to their bulk, surface properties are of great importance and SAMs are routinely used to obtain desired surface functionalisations.

SAMs consist of organic molecules which form ordered films when adsorbed to solids. The individual molecules consist of a hydrophilic head group with a high affinity for a particular substrate and a hydrophobic carbon backbone terminated by a functional group as shown

in Figure 5 (a). In a specific application, the head group is chosen to match the used substrate material, whereas the functional group and backbone length are chosen based on the intended properties of the coated surface⁴⁸. A variety of head group/backbone/functional group combinations are commercially available.

In this thesis, the alkanethiol 1H,1H,2H,2H-Perfluorodecanethiol illustrated in Figure 5 (b) was used in papers II and III to modify the surfaces of produced structures. Its head consists of a thiol group which readily adsorbs to gold, silver, copper⁴⁹, palladium⁵⁰, or platinum⁵¹. No special functional group was required, as the low surface energy was already provided by the fluorinated backbone. In paper IV, the alkanethiol 11-Amino-1-undecanethiol was used to increase the wetting of the functionalised nanowires by SU-8. Its terminal amino group might also be used to add a positive surface charge to the nanowires in order to adsorb DNA.

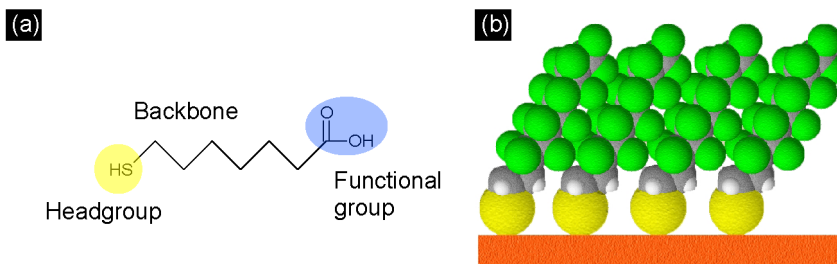


Figure 5: Composition of self assembled monolayers (a): Sketch of an alkanethiol (functionalised with a carboxyl group), (b): Sketch of a SAM of 1H,1H,2H,2H-Perfluorodecanethiol as used in paper II and III

In contrast to the deposition on Cu, the functionalisation of CuO by alkanethiols has been described based on a two step reaction resulting in monolayers⁵² or multilayers⁵³. Our own observations suggesting a multilayer assembly are described in paper III.

2.3 Superhydrophobic surfaces

Superhydrophobic surfaces are commonly classified by having a water contact angle larger than 150° ⁵⁴. A popular example from nature is the leaf of the lotus flower, which achieves contact angles above 160° ⁵⁵.

Superhydrophobic surfaces combine a low surface energy with a micro and/or nanoscale roughness. The lotus flower realises this by forming a microrough structure composed of epidermal cells covered with a nanorough structure of hydrophobic crystalline waxes⁵⁶. For artificial superhydrophobic surfaces, a variety of fabrication schemes have been reported. They are based either on the roughening or self assembly of low surface energy materials or on the fabrication of rough surfaces, which are subsequently coated with a low surface energy functional layer⁵⁷.

Depending on how the surface is wetted, several idealised states differing in water contact angle and droplet mobility can be identified as shown in Figure 6.

In this thesis, water droplets in the Cassie and Lotus state are examined (see Figure 6(d) and (e)). In contrast to those in Wenzel state, these droplets float on pockets of air trapped underneath them, resulting in a very low contact angle hysteresis and a correspondingly high droplet mobility.

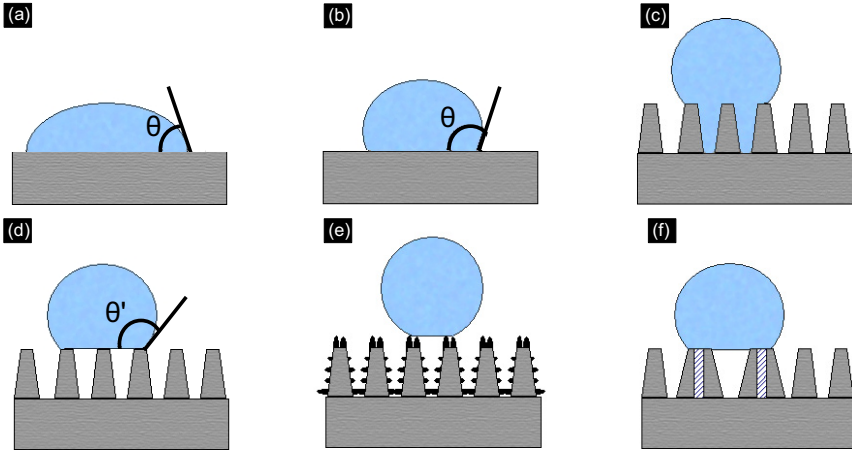


Figure 6: Different surface/liquid-droplet interactions after⁵⁴. (a): A hydrophilic surface (contact angle $\theta < 90^\circ$), (b): A hydrophobic surface ($\theta > 90^\circ$), (c): A suberhydrophobic surface with a droplet in Wenzel state, (d): A suberhydrophobic surface with a droplet in Cassie state (with an apparent contact angle $\theta' > 150^\circ$), (e): A suberhydrophobic surface with a droplet in Lotus state (special case of Cassie state with two scale roughness), (f): A suberhydrophobic surface with a droplet in Gecko state (special case of Cassie state, hatched areas are filled with air but without connection to the atmosphere)

The apparent contact angle θ' of a water droplet in the Cassie state can be calculated according to the Cassie-Baxter model⁵⁸. It depends on the surface roughness in form of the fraction ϕ_s of the fluid-solid interface in comparison to the total apparent contact area and the surface chemistry in form of the contact angle of water on a flat surface of the same material θ :

$$\cos(\theta') = \phi_s(1 + \cos \theta) - 1$$

As can be seen, a high contact angle requires both a high surface roughness corresponding to a low value of ϕ_s and a low surface energy corresponding to a high value of θ . This was realised in paper III

by the formation of a microrough copper surface coated with a self assembled monolayer of fluorocarbons. Additionally, CuO nanowires were grown on the rough Cu surface to produce a lotus like surface with two-scale roughness (without a direct effect on the contact angle, as it approached 180° already for the Cu substrate).

The high mobility of water droplets on the surfaces was then used to fabricate a digital microfluidic system.

2.4 Digital microfluidics

In digital microfluidic devices, droplets of fixed, small volumes are mixed and analysed (hence the name in analogy to digital electronics). In closed systems, this can be realised by using two non mixable fluids, e.g. a water based phase in oil⁵⁹, whereas open systems rely on the formation of self-confined droplets on a hydrophobic surface. Generally, surface based systems offer a higher flexibility in droplet handling, whereas closed systems offer higher throughputs.

Most of the research in surface based systems is done on flat, hydrophobic surfaces fitted with isolated electrodes. When an electrode is switched on, the electric field lowers the hydrophobicity of the isolation layer on top of it. This phenomenon termed electrowetting on dielectric can be used to move droplets, which are in between switching electrodes⁶⁰.

Superhydrophobic surfaces offer complementary droplet manipulation methods, due to the higher mobility of water droplets on them. This includes the use of magnetic fields in combination with liquids containing magnetic microparticles⁶¹ or direct physical contact with a guiding wire⁶².

Wire guidance is used in paper III with an optical fibre in an approach to produce a superhydrophobicity based digital microfluidic system.

2.5 Nanostructure cell-impalement

The use of nanowires to impale cells has recently developed into an alternative transfection method^{63,64,15}. Transfection is the process of introducing foreign compounds (mostly genetic material such as DNA

or RNA but also e.g. proteins or quantum dots) into living cells. The term is mostly used for non-viral systems applied to cultured cells. In transfection systems based on impalement of the cells, the transport across the cell membrane is realised by first attaching the target compounds to the wire surface or depositing them within the tubes and then releasing them, once the nanostructures spiked into the cells.

Due to the much smaller diameter of the nanowires compared to the cells, it is possible for cells to rearrange their cell membrane and organise internally around the wires and to grow on the surface while being impaled^{14,65}.

Research on vertical nanowires attached to a surface is complemented by studies on single nanostructure/cell interactions using nanowires or nanotubes attached to AFM cantilevers^{66,13}. In the later study, it was shown, that carbon based nanoneedles with diameters of 30 – 40 nm could penetrate through the cell membrane to break into the interior of adherent cells after an indentation depth of only 100 – 200 nm.

Nanowire and nanotube based transfection systems are still in an early, experimental phase, but they are expected to develop into valuable alternatives to conventional methods, especially for cell types, which are presently hard to transfect¹⁵. Additionally, the fact that target compounds are first deposited and subsequently transported into seeded cells, makes such systems a preferential approach for reverse transfection cell arrays (The name “reverse transfection” derives from the reverse order of introducing cells and e.g. DNA compared to the conventional procedure: The DNA is deposited on the surface, before adherent cells are allowed to grow on it. For conventional reverse transfection procedures, this is realised by immobilizing a DNA/transfection agent mixture in a gelatin matrix on a glass slide⁶⁷).

3 Summary of the papers

3.1 Paper I

This paper describes how the bristles of the marine worm *Aphrodita Aculeata* (sea mouse) can be used as key components in a nanoporous template. These templates were then used to produce nanowires and nanotubes using standard template based nanofabrication techniques.

As a consequence of their biosynthesis, bristles of sea mice are composed of a regular array of nanochannels in a chitin/protein matrix. As the channels span through the whole bristle (reaching up to two centimetres in length), the aspect ratio of the produced nanostructures could be substantially increased in comparison to structures made in more conventional, membrane based templates. In the paper, the bristles are characterized and a preparation procedure is described to fabricate nickel and copper nanowires by electrodeposition and aluminium oxide nanotubes by atomic layer deposition. Finally, two different approaches to separate the produced wires or tubes from the biotemplate are presented and discussed.

3.2 Paper II

The paper describes a simple way to create and pattern defect free arrays of CuO nanowires by oxidizing copper foils in a standard laboratory oven. Commonly, the large surface mismatch between copper and its oxides and the corresponding stress at the copper/copper oxide interface results in flakes of nanowire-covered oxide layers detaching from the sample. It is shown in the paper that the use of thin foils as substrates allows to fabricate nanowire covered surfaces without the characteristic flaking problem.

Additionally, two procedures to topographically and spatially pattern the samples are presented alongside with some potential applications for the produced nanowire arrays.

3.3 Paper III

In this paper a digital microfluidic system based on a superhydrophobic surface is presented. The roughness required for a surface to be superhydrophobic is produced by etching a polycrystalline copper sample to expose its grains as well as by subsequently decorating it with CuO nanowires (to achieve a two scale micro and nanorough surface). A self assembled layer of fluorocarbons is then deposited on the surfaces to obtain the necessary low surface energy. Based on these superhydrophobic surfaces, a digital microfluidic system with components to create, move, and store droplets is presented.

3.4 Paper IV

This paper, which is under preparation, describes a composite SU-8/CuO nanowire system, which is intended to be used to transfect cells by impalement. The system is based on the CuO nanowire fabrication procedure described in paper II and allows to make vertically aligned arrays of either gold coated nanowires or hollow nanoneedles on an SU-8 membrane.

After fabrication, the arrays were interfaced with HeLa cells and it could be shown that the cells attach and spread on the nanostructured surface. The authors intend to use the system together with adopted, published procedures to deposit target materials such as DNA on the nanowires or in the nanotubes in order to transport it across the cell membrane by impaling the cells.

4 General discussion

This discussion is intended to expand on the discussions given in the individual papers by focussing more on the general picture and by pointing out the advantages and drawbacks of the applied methods in comparison to alternative procedures. First, the use of sea mouse spines as high aspect ratio nanoporous templates, followed by a closer look at the potential of CuO nanowire arrays to be used together with biological systems.

4.1 The sea mouse based nanoporous template

It was shown in paper one, that the regular arrays of nanochannels, which are responsible for the iridescent appearance of the sea mouse spine (by making it a photonic crystal²⁴) can be used to produce nanotubes and nanowires using established fabrication methods.

In contrast to other nanoporous templates such as porous anodic alumina and track-etched polycarbonate membranes¹⁷, which are produced by introducing pores into a solid material, the nanochannels in the sea mouse spine need no further preparation procedures, as they are a consequence of the spine's biosynthesis. However, as the channels are concealed within the interior of the spines, it was first necessary to develop a suitable way to open the spines without deforming them. This was found to be possible using microtomy or a simple breaking procedure for spines cooled in liquid nitrogen. As the latter method was much simpler to implement, it was used throughout all the experiments. It also resulted in spines embedded in epoxy, which made it possible to further process the template assembly in analogy to conventional membrane-based templates, and to directly adopt deposition procedures developed for them.

The main obstacle for practical applications of nanostructures produced in sea mouse spines and the severest deviation from processes developed for conventional templates turned out to be the remarkable toughness of the spine, which made it difficult to decompose the template and to free the nanostructures fabricated within it. The spines showed to be resistant to decomposition over a wide range of pH values (pH 1 to pH 10 for a week at room temperature) and temperatures

(up to 200 °C), which on the one hand makes it possible to use a wide range of deposition parameters to make nanotubes or nanowires, but simultaneously requires harsh, potentially damaging, conditions to free them from the template. This conflict has so far not been resolved for wires spanning through the whole millimetre long template.

Consequently, the maximum length of nanostructures, which can be fabricated and isolated in a sea mouse spine based template is presently not limited by the physical structure of the template, but by its chemical composition. Using the decomposition methods described in the article, the maximum length of nanowires separated from the template was on the order of 100 to 200 μm .

A promising future approach is to look more closely at the composition of the spines and make use of their biological origin. As all polychaeta bristles, the sea mouse spine is made of a chitin/protein composite⁶⁸. This should, in principle, make it possible to decompose its structure with the help of chitinases (chitin degrading enzymes present in plants, insects, crustaceans, microorganisms as well as some mammals and fish⁶⁹) and proteases (protein degrading enzymes present in all organisms).

Alternatively, as the fabrication procedure of all polychaeta bristles, and thus the presence of channels within them is similar, one can aim to deposit nanostructures in bristles, with a different material composition making them easier to decompose.

4.2 Interaction of CuO nanowires and biological systems

As CuO is a p-type, direct, narrow band gap semiconductor, CuO nanowires have potential applications in a variety of fields apart from the nano-biosciences, such as in sensing⁷⁰ or as field emitters⁴⁷. Even though the mechanism to produce defect-free arrays on CuO nanowires without the characteristic flaking problem presented in paper II might be advantageous to all these applications, this discussion will be limited on the potentials of using CuO nanowires in biology-related setups.

The use of semiconductor nanowires in biology, especially as a tool for crossing the cell membrane in a minimal invasive way, was recently

highlighted in a Nano Letters perspective article on the future of semiconductor nanowires⁷¹. The same article advocates to focus developments in the field equally strong on improving existing applications as on developing new ones, even though “yes-or-no” findings receive a broader recognition than those focusing on “better-or-worse”.

When aiming to transport target compounds across the cell membrane, the use of CuO nanowires might improve already demonstrated methods according to the “better-or-worse” approach, as its advantages might outweigh its limitations: The main advantage of CuO nanowires compared to alternative approaches such as those using carbon nanofibers⁶⁴ or silicon nanowires¹⁵ is the ease of their fabrication from a comparatively cheap source material. The resulting abundance of nanowire covered substrates is a major advantage on the route to developing nanowire arrays into working devices.

Their main disadvantage is the comparatively low degree of control which the researcher has over the nanowires’ position, diameter, and length. Whereas these limits severely affect the applicability of CuO nanowires in a variety of fields, they play less of a roll in cell impalement (as long as the wires do not exceed a critical diameter and reach an acceptable average length and density) or the fabrication of superhydrophobic surfaces. Also the cracks, which are buried at the Cu/Cu₂O interface might limit the applicability of surfaces grown according to the procedure presented in paper II, as they might impair the electrical conductivity across the assembly.

In the context, in which the wires were used in this thesis, this is not an issue, as no electrical measurements have been conducted. Here, the cracks between the Cu and Cu₂O layer were actually an advantage, as they made it possible to peel off the Cu layer from polymer based devices as done in paper IV.

Additionally, using thin copper sheets as substrates makes processing of the nanowire arrays rather simple, as the substrate can be cut into smaller pieces using tweezers and easily removed using HCl or a CuCl₂ based etch solution⁷². The latter is especially important when the nanowires are intended to serve as moulds for SU-8 based devices as the chemistry to remove the CuO wires or the Cu substrate leaves the SU-8 unaffected.

The integration of an SU-8 layer also offers the possibility to have

a dedicatedly different surface composition at the nanowires (gold) compared to their surrounding (SU-8). Using e.g. SAMs to specifically adsorb target compounds to the wires, this is an advantage over conventional systems, where such compounds adsorb at all surfaces, as the wires are often made out of the same material as their support¹⁵ or the whole assembly is sputter coated prior to functionalisation⁶⁴.

CuO nanowires could also be used to fabricate superhydrophobic surfaces. They were used in paper III to add an extra layer of nanometer scale roughness on top of the micrometer scale roughness produced by the copper grains. The reason, why no flaking was observed on the grainy copper surface was probably that a thickness relation similar to that given in paper II developed within the individual copper grains at the sample's surface, resulting in cracks being buried inside the substrate. However, the degree of control of flaking on the etched plates used in paper III was much lower than on the thin foils of paper II.

Investigating the static water contact angles of the micrometer-rough surface made of copper grains and the micro and nanometre-rough surface made of oxidized and nanowire decorated copper grains, no differences could be seen, as already the 1H,1H,2H,2H-Perfluorodecanethiol functionalised copper surface showed very high contact angles close to 180°. This is an advantage of man made superhydrophobic structures over biological ones: As can be seen from the Cassie model given in Section 2.3, the total apparent contact angle is a combination of the surface roughness and the contact angle on a flat surface of the same material (and thus the material's surface energy). As nature is basically limited to use low energy surface coverings made of carbon and hydrogen it needs to improve the surface roughness to reach very high contact angles (as e.g. done by the lotus flower).

As artificial superhydrophobic surfaces can make use of lower surface energy fluorocarbons, they can often reach or surpass contact angles on biological surfaces without having two scale rough surface features. Nevertheless, such features might be important when dynamic processes, such as droplet impacts on the surfaces are considered.

5 Conclusions and Outlook

Different ways to produce high aspect ratio nanostructures were evaluated in this thesis. First, an unconventional template based on the spines of the sea mouse was used to produce nanowires and nanotubes with lengths, which cannot be obtained with standard templates. The fabrication procedure involved a considerable amount of manual, serial steps, and some issues in template decomposition remain to be solved. Nevertheless, sea mice based templates offer the possibility to produce high aspect ratio nanostructures of a relatively wide range of materials and might be used in experiments, where small amounts of long nanowires or nanotubes are needed, which cannot be made using simpler methods. They might also be useful for applications in which the nanostructures are used in arrays and are not separated from the template they grew in. Examples might include the study of heat conductance along arrayed, long nanowires or tubes⁷³ or fluid transport through tubes deposited inside the spine for filtering applications⁷⁴. Additionally, adopting the procedures presented in paper I nanowires and nanotubes with different geometries (e.g. hook shaped) might be produced inside the bristles of other polychaeta species.

In addition to the work on sea mouse bristles, a procedure how non-flaking CuO nanowire arrays could be easily produced on large areas was described in this thesis and two applications of these nanowire arrays were investigated. The described devices were produced from comparatively cheap materials using relatively simple fabrication procedures. Low costs are especially an advantage for nanostructured surfaces applied in biological research, as the sensitivity of many biological systems to contamination often requires single use devices. Furthermore, nanowire fabrication was combined with standard lithography methods, which might ease the integration of the nanowires into top-down microfabricated systems.

The procedures and devices presented in papers II to IV might be adopted in future developments in a variety of fields. As high surface area CuO structures can be used as catalysts^{75,76}, the procedures described in paper II for nanowire growth and substrate patterning by moulding as well as those described in paper III for substrate patterning by etching and electrodeposition might be of direct use in

catalytic applications of CuO. Additionally, nanowires of different materials are used as supports for catalyst (which are e.g. deposited by ALD). Such setups might benefit from using CuO nanowires instead of performance limiting, very dense nanowire arrays produced in AAO membranes⁷⁷. Finally, one can imagine how almost arbitrary shaped macroscopic nanowire covered objects can be created by origami-like folding of thin copper foils followed by oxidative CuO nanowire growth.

Based on paper IV, the combination of CuO nanowires with SU-8 might have several future applications both inside and outside of biotechnology. When the Cu and Cu₂O layer are removed from the backside of a sample consisting of CuO nanowires embedded in SU-8, direct electrical contact to the nanowires can be made on both sides (as they reach from the bottom of the CuO layer through the SU-8). This might e.g. be used to produce CuO nanowire based LEDs⁷⁸. Regarding future bio-applications, the integration of SU-8 might ease the use of the nanowire arrays as parts of microfluidic devices and the comparatively low cost associated with the SU-8/CuO nanowire system might favour its application in array based high throughput screening procedures e.g. in cell biology research.

Considering the CuO nanowire derived SU-8 nanoneedles presented in paper IV, the integration in a microfluidic system might allow to inject and extract material from a variety of impaled structures. While ultimately directed towards the direct access to the cytoplasm of living cells, the same approach might also be used to transfer cargo into more robust, medically important compounds such as liposomes⁷⁹ or erythrocyte ghosts⁸⁰.

References

1. Gao, X. and Matsui, H. *Adv. Mater.* **17**(17), 2037–2050 (2005).
2. Rothmund, P. *Nature* **440**(7082), 297–302 (2006).
3. Seeman, N. *Annu. Rev. Biochem.* **79**, 65–87 (2010).
4. Rechtes, M. and Gazit, E. *Science* **300**(5619), 625 (2003).
5. Zhou, Y. and Shimizu, T. *Chem. Mater* **20**(3), 625–633 (2008).
6. Knez, M., Bittner, A., Boes, F., Wege, C., Jeske, H., Maiß, E., and Kern, K. *Nano Lett.* **3**(8), 1079–1082 (2003).
7. Meller, A., Nivon, L., Brandin, E., Golovchenko, J., and Branton, D. *Proc. Natl. Acad. Sci. USA* **97**(3), 1079 (2000).
8. Soong, R., Bachand, G., Neves, H., Olkhovets, A., Craighead, H., and Montemagno, C. *Science* **290**(5496), 1555 (2000).
9. Zheng, G., Patolsky, F., Cui, Y., Wang, W., and Lieber, C. *Nat. Biotechnol.* **23**(10), 1294–1301 (2005).
10. Patolsky, F. and Lieber, C. *Materials Today* **8**(4), 20–28 (2005).
11. Tegenfeldt, J., Prinz, C., Cao, H., Huang, R., Austin, R., Chou, S., Cox, E., and Sturm, J. *Anal. Bioanal. Chem.* **378**(7), 1678–1692 (2004).
12. Fan, R., Karnik, R., Yue, M., Li, D., Majumdar, A., and Yang, P. *Nano Lett.* **5**(9), 1633–1637 (2005).
13. Vakarelski, I., Brown, S., Higashitani, K., and Moudgil, B. *Langmuir* **23**(22), 10893–10896 (2007).
14. Pearton, S., Lele, T., Tseng, Y., and Ren, F. *Trends Biotechnol.* **25**(11), 481–482 (2007).

15. Shalek, A., Robinson, J., Karp, E., Lee, J., Ahn, D., Yoon, M., Sutton, A., Jorgolli, M., Gertner, R., Gujral, T., et al. *Proc. Natl. Acad. Sci. USA* **107**(5), 1870 (2010).
16. Hoshino, T., Konno, T., Ishihara, K., and Morishima, K. *Biomedical Robotics and Biomechatronics, 2008. 2nd IEEE RAS EMBS International Conference on* , 506–510 oct. (2008).
17. Cao, G. and Liu, D. *Adv. Colloid Interface Sci.* **136**(1-2), 45–64 (2008).
18. Adelung, R., Aktas, O., Franc, J., Biswas, A., Kunz, R., Elbahri, M., Kanzow, J., Schürmann, U., and Faupel, F. *Nat. Mater.* **3**(6), 375–379 (2004).
19. Zach, M., Inazu, K., Ng, K., Hemminger, J., and Penner, R. *Chem. Mater* **14**(7), 3206–3216 (2002).
20. Sanchez, C., Arribart, H., and Guille, M. *Nat. Mater.* **4**(4), 277–288 (2005).
21. Deville, S., Saiz, E., Nalla, R., and Tomsia, A. *Science* **311**(5760), 515 (2006).
22. Huang, J., Wang, X., and Wang, Z. *Nanotechnology* **19**, 025602 (2008).
23. Gazit, E. *FEBS J.* **274**(2), 317–322 (2007).
24. Parker, A., McPhedran, R., McKenzie, D., Botten, L., and Nicorovici, N. *Nature* , 36–36 (2001).
25. Enculescu, I., Siwy, Z., Dobrev, D., Trautmann, C., Toimil Molares, M., Neumann, R., Hjort, K., Westerberg, L., and Spohr, R. *Appl. Phys. A- Mater.* **77**(6), 751–755 (2003).
26. Pan, H., Liu, B., Yi, J., Poh, C., Lim, S., Ding, J., Feng, Y., Huan, C., and Lin, J. *J. Phys. Chem. B* **109**(8), 3094–3098 (2005).
27. Shin, H., Dong, J., and Liu, M. *Adv. Mater.* **15**(19), 1610–1614 (2003).

28. Lou, H. and Huang, Y. L. *Electroplating, in Encyclopedia of chemical processing*. CRC, (2005).
29. Leskelä, M. and Ritala, M. *Thin Solid Films* **409**(1), 138–146 (2002).
30. Dillon, A., Ott, A., Way, J., and George, S. *Surf. Sci.* **322**(1-3), 230–242 (1995).
31. Law, M., Goldberger, J., and Yang, P. *Ann. Rev. Mater. Res.* **34**(1), 83 (2004).
32. She, G., Zhang, X., Shi, W., Fan, X., Chang, J., Lee, C., Lee, S., and Liu, C. *Appl. Phys. Lett.* **92**, 053111 (2008).
33. Sun, Y., Yin, Y., Mayers, B., Herricks, T., and Xia, Y. *Chem. Mater* **14**(11), 4736–4745 (2002).
34. Jiang, X., Herricks, T., and Xia, Y. *Nano Lett.* **2**(12), 1333–1338 (2002).
35. Wen, X., Wang, S., Ding, Y., Wang, Z., and Yang, S. *J. Phys. Chem. B* **109**(1), 215–220 (2005).
36. Dong, Z., Fu, Y., Han, Q., XU, Y., and Zhang, H. *J. Phys. Chem. C* **111**(50), 18475–18478 (2007).
37. Fan, H., Scholz, R., Kolb, F., and Zacharias, M. *Appl. Phys. Lett.* **85**, 4142 (2004).
38. Rackauskas, S., Nasibulin, A., Jiang, H., Tian, Y., Kleshch, V., Sainio, J., Obraztsova, E., Bokova, S., Obraztsov, A., and Kauppinen, E. *Nanotechnology* **20**, 165603 (2009).
39. Hansen, B., Lu, G., and Chen, J. *J. Nanomater.* **2008**(1), 20 (2008).
40. Huang, L., Yang, S., Li, T., Gu, B., Du, Y., Lu, Y., and Shi, S. *J. Cryst. Growth* **260**(1-2), 130–135 (2004).
41. Kumar, A., Srivastava, A., Tiwari, P., and Nandedkar, R. *J. Phys.: Condens. Matter* **16**, 8531 (2004).

42. Xu, C., Woo, C., and Shi, S. *Chem. Phys. Lett.* **399**(1-3), 62–66 (2004).
43. Gonçalves, A., Campos, L., Ferlauto, A., and Lacerda, R. *J. Appl. Phys.* **106**, 034303 (2009).
44. Li, X., Zhang, J., Yuan, Y., Liao, L., and Pan, C. *J. Appl. Phys.* **108**, 024308 (2010).
45. Nasibulin, A., Rackauskas, S., Jiang, H., Tian, Y., Mudimela, P., Shandakov, S., Nasibulina, L., Jani, S., and Kauppinen, E. *Nano Research* **2**(5), 373–379 (2009).
46. Zhang, K., Rossi, C., Tenailleau, C., Alphonse, P., and Chané-Ching, J. *Nanotechnology* **18**, 275607 (2007).
47. Wang, R. and Li, C. *Cryst. growth des.* **9**(5), 2229–2234 (2009).
48. Love, J., Estroff, L., Kriebel, J., Nuzzo, R., and Whitesides, G. *Chem. Rev* **105**(4), 1103–1170 (2005).
49. Laibinis, P., Whitesides, G., Allara, D., Tao, Y., Parikh, A., and Nuzzo, R. *J. Am. Chem. Soc.* **113**(19), 7152–7167 (1991).
50. Carvalho, A., Geissler, M., Schmid, H., Michel, B., and Delamarque, E. *Langmuir* **18**(6), 2406–2412 (2002).
51. Li, Z., Chang, S., and Williams, R. *Langmuir* **19**(17), 6744–6749 (2003).
52. Sung, M., Sung, K., Kim, C., Lee, S., and Kim, Y. *J. Phys. Chem. B* **104**(10), 2273–2277 (2000).
53. Keller, H., Simak, P., Schrepp, W., and Dembowski, J. *Thin Solid Films* **244**(1-2), 799–805 (1994).
54. Wang, S. and Jiang, L. *Adv. Mater.* **19**(21), 3423–3424 (2007).
55. Cheng, Y., Rodak, D., Wong, C., and Hayden, C. *Nanotechnology* **17**(5), 1359–1362 (2006).
56. Barthlott, W. and Neinhuis, C. *Planta* **202**(1), 1–8 (1997).

57. Roach, P., Shirtcliffe, N., and Newton, M. *Soft Matter* **4**, 224–240 (2007).
58. Cassie, A. and Baxter, S. *Trans Faraday Soc* **40**, 546–551 (1944).
59. Huebner, A., Sharma, S., Srisa-Art, M., Hollfelder, F., Edel, J., and demello, A. *Lab Chip* **8**(8), 1244–1254 (2008).
60. Fair, R., Khlystov, A., Tailor, T., Ivanov, V., Evans, R., Griffin, P., Srinivasan, V., Pamula, V., Pollack, M., and Zhou, J. *IEEE Des. Test Comput.* **24**(1), 10–24 (2007).
61. Egatz-Gómez, A., Schneider, J., Aella, P., Yang, D., Domínguez-García, P., Lindsay, S., Picraux, S., Rubio, M., Melle, S., Marquez, M., et al. *Appl. Surf. Sci.* **254**(1), 330–334 (2007).
62. Jeong-Yeol, Y. and David, Y. *J Biol Eng* **2**, 15 (2008).
63. Kim, W., Ng, J., Kunitake, M., Conklin, B., and Yang, P. *J. Am. Chem. Soc* **129**(23), 7228–7229 (2007).
64. Peckys, D., Melechko, A., Simpson, M., and McKnight, T. *Nanotechnology* **20**, 145304 (2009).
65. Berthing, T., Sørensen, C., Nygard, J., and Martinez, K. *J. Nanoneurosci.* **1**(1), 3–9 (2009).
66. Obataya, I., Nakamura, C., Han, S., Nakamura, N., and Miyake, J. *Nano Lett.* **5**(1), 27–30 (2005).
67. Wu, R., Bailey, S., and Sabatini, D. *Trends cell biol.* **12**(10), 485–488 (2002).
68. Hausen, H. *Hydrobiologia* **535**(1), 37–52 (2005).
69. Koga, D., Mitsutomi, M., Kono, M., and Matsumiya, M. *Chitin and chitinases* , 111–123 (1999).
70. Hansen, B., Kouklin, N., Lu, G., Lin, I., Chen, J., and Zhang, X. *J. Phys. Chem. C* **114** (6), 2440–2447 (2010).

71. Yang, P., Yan, R., and Fardy, M. *Nano Lett.* **10**(5), 1529–1536 (2010).
72. Cakir, O. *J Mater Process Tech* **175**(1-3), 63–68 (2006).
73. Menke, E., Brown, M., Li, Q., Hemminger, J., and Penner, R. *Langmuir* **22**(25), 10564–10574 (2006).
74. Han, J., Fu, J., and Schoch, R. *Lab Chip* **8**(1), 23 (2008).
75. Bandara, J., Guasaquillo, I., Bowen, P., Soare, L., Jardim, W., and Kiwi, J. *Langmuir* **21**(18), 8554–8559 (2005).
76. Feng, Y. and Zheng, X. *Nano Lett.* , 567–577.
77. Kemell, M., Pore, V., Tupala, J., Ritala, M., and Leskelä, M. *Chem. Mater* **19**(7), 1816–1820 (2007).
78. Könenkamp, R., Word, R., and Schlegel, C. *Appl. Phys. Lett.* **85**, 6004 (2004).
79. Jesorka, A. and Orwar, O. *Analytical Chemistry* **1** (2008).
80. Byun, H., Suh, D., Yoon, H., Kim, J., Choi, H., Kim, W., Ko, J., and Oh, Y. *Gene ther.* **11**(5), 492–496 (2004).

6 Paper I

Is not included due to copyright

7 Paper II

Oxidative Fabrication of Patterned, Large, Defect-Free CuO Nanowire arrays

F. Mumm and P. Sikorski

Department of Physics, Norwegian University of Science and Technology, Trondheim,
Norway

E-mail: pawel.sikorski@phys.ntnu.no, mumm@phys.ntnu.no

Abstract. We report a simple and fast approach to fabricate large, defect free arrays of CuO nanowires by oxidizing thin copper substrates in air. Oxidative CuO nanowire growth is commonly accompanied by oxide layer flaking due to stress at the copper - copper oxide interface. Using thin substrates is shown to prevent this flaking by introducing favourable material thickness ratios in the samples after oxidation. Additionally, thin foils allow larger scale topographic patterns to be transferred from an underlying mould to realise non-flat, nanowire decorated surfaces. Further patterning is possible by electrodeposition of a nickel layer, which restricts nanowire growth to specific areas of the sample.

1. Introduction

Copper oxide nanowires can be remarkably easily fabricated in form of large scale vertically aligned arrays by heating copper substrates in air [1] with applications including e.g. field emitters [2], gas sensors[3], or superhydrophobic surfaces [4]. As the fabrication procedure is so simple, CuO nanowires are also convenient for experiments, in which nanowires made of rather arbitrary materials can be used[5, 6, 7].

The wires form spontaneously and catalyst free during the oxidation of copper substrates at temperatures ranging roughly from 400 °C to 700 °C[1], with a nanowire density increasing with the oxygen partial pressure [8]. After the oxidation, the CuO wires build the top part of an oxide layer system of cupric oxide (CuO) and cuprous oxide (Cu₂O) on copper. The oxide layer thicknesses are usually in the range of a few microns. The wires themselves are single crystalline, p-type semiconductors with a bandgap of about 1.4 eV [3], strong photoluminescence [9], a diameter varying broadly around 100 nm, and a length of up to 20 μm [1].

Due to the large surface mismatch between copper and Cu₂O, flaking of the oxide layers from the copper substrate is a common problem in the production of nanowire covered CuO surfaces[10, 11]. A first method to prevent flaking was presented by Zhang et al.[10], who used lithographic patterning to form separated copper patches on a silicon substrate. After the oxidation, the discontinuous surface allowed stress release at the edges and, thus, prevented the oxide layers from detaching.

Another approach was recently introduced by Wang and Li[11], who demonstrated that flaking could be prevented by incubating the substrates in a zinc nitrate containing solution for several hours to deposit a micrometer layer of porous ZnO on top of the copper. During oxidation, the ZnO layer caused all generated Cu₂O to further react to CuO, of which only a small film directly contacted the copper substrate. This reduced the misfit stress and prevented the formation of cracks.

Here we present a simple and quick alternative method to prepare non-flaking CuO nanowire arrays, based on using very thin copper foils (25 μm, 99.98 % copper, obtained from Sigma Aldrich). When heating such thin foils, the thickness of the forming oxide layers substantially exceeds the thickness of the remaining copper substrate as shown in Figure 1(e). In contrast to commonly used thicker samples, this causes the misfit stress

to relax mostly by deforming the remaining substrate sandwiched within the foil, while leaving the oxide layers intact. As only the oxide layers interface with the outside world, the resulting CuO surface shows large area, defect free nanowire coverage with a dark black appearance as illustrated in Figure 1 (see also Figure 2 in the supporting material).

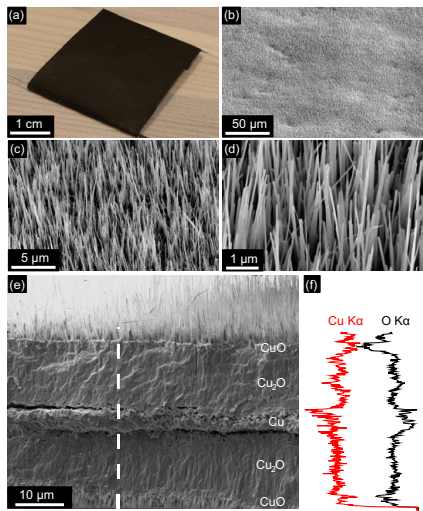


Figure 1. Nanowire decorated flat surface: (a): Oxidized foil fixed around a glass slide, (b)-(d): Different magnifications of the surface, (e): Cross section showing oxide layers and remaining substrate, (f): EDX spectrum in arbitrary counts along the dashed line in (e)

2. Nanowire Growth and Patterning

As received copper foils were cut in pieces of about 2.5 x 3.5 cm and cleaned by subsequently washing them in 2 M HCl, DI water, acetone and ethanol in an ultrasonic bath followed by drying using wipes. The cleaned foils were then folded around microscopy slides and any irregularities in the original foil were flattened out by rubbing a rumpled wipe over the surface.

Nanowires were grown by placing the microscope slide/ copper foil assembly on a second glass slide and inserting those quickly in a laboratory oven (Carbolite CWF 1200) already heated to 500 °C. After two hours of incubation, the glass slides were removed from the oven and allowed to quickly cool down to room temperature on a heat resistive surface covered by a glass dish. For properly cleaned thin foils, no flaking was observed. In contrast, using the same procedure with thicker samples, resulted in considerable flaking as shown in the supplementary material. The growth of defect-free nanowire arrays on thin enough substrates might also provide an explanation why flaking is commonly not mentioned in articles based on oxidized copper TEM grids[1, 9].

Contrary to thick Cu substrates, the thin foils could bend in reaction to inhomogeneous thermal expansion or stress created in the oxidation process. It was observed that increased macroscopic flexibility resulted in a less dense nanowire coverage, which could be used to tune the density of the nanowires on the oxidized surface as shown in the supplementary material. This is consistent with a model of nanowire growth, attributing the growth process to stress relaxation at the CuO/Cu₂O interface[12]. In order to minimize the ability of the used foils to bend, and thus to maximize the nanowire density, flattened foils were tightly folded around microscope slides prior to oxidation.

After oxidation, the nanowire covered foils could be handled with tweezers and cut into smaller pieces using scissors. This commonly resulted in some flaking along the cutting edges as visible in Figure 3(a) for samples where the flaps fixing them around the glass slides were cut off. The flakes further indicate, that cracks formed along the Cu/ Cu₂O interface but did not notably span across the oxide layers to the surface of the foils. This is in contrast to the more complex sample preparation by ZnO deposition, where cracks were avoided and cutting could be performed without flaking[11].

Using thin foils additionally offers the possibility to add macroscopic topography to the samples by structuring the foils on a macroscopic mould instead of a flat glass slide. As a demonstration, various millimetre scale moulds such as a regular array of plastic spikes (with a foil which was subsequently turned around to produce dimples), a metal spiral pattern, and a Lego brick were used as shown in Figure 2. The resolution of this approach is on the order on about hundred micrometer, given by the thickness of the foil and the topography of the moulds. However, for suitable moulds, this simple pattern transfer mechanism might be a quick alternative to more complex approaches such as lithography and etching.

When using moulds to shape the substrates prior to oxidation, the patterned foils are often less stretched than flat ones, resulting in a lower density of nanowire coverage as seen in Figure 2.

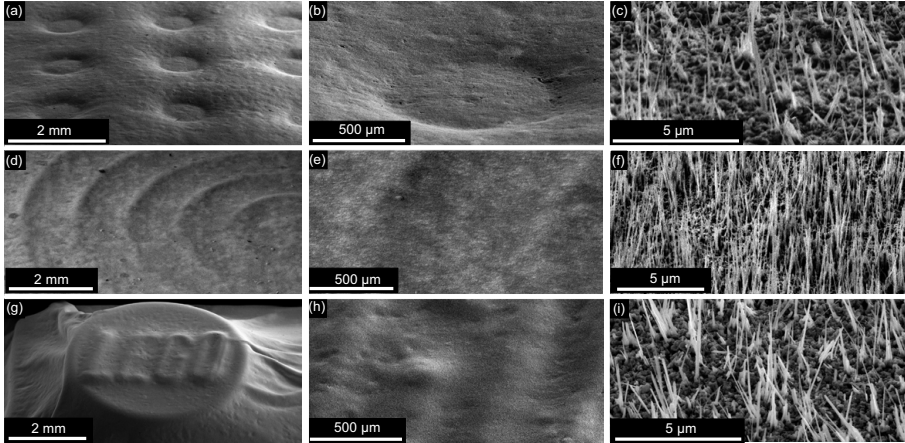


Figure 2. Nanowire decorated surfaces shaped after different moulds: (a)-(c): Dimple array, (d)-(f): Spiral, (g)-(i): Lego brick

In addition to growing homogeneous nanowire arrays either on flat or on structured surfaces, it is also possible to constrain their formation to selected areas resulting in a surface topography similar to the one presented by Zhang et al.[10]. Whereas nanowire growth is selectively enabled by Cu deposition on Si in their approach, it is selectively restricted in our's. This is done by placing a mask on the stretched out Cu foils followed by the electrodeposition of Ni around it. After mask removal, the Ni layer serves as an oxidation barrier for the underlying Cu during the heating of the sample. Consequently, the formation of CuO nanowires is restricted to areas without Ni coating, i.e. those which were priorly covered by the mask.

For this approach, Ni was electrodeposited on the stretched out copper foils from an electrolyte of 240 g/l $\text{NiSO}_4 \cdot 6\text{H}_2\text{O}$, 25 g/l NiCl_2 , and 50 g/l H_3BO_3 at a potential of -2.5 V for 15 minutes using a two electrode electrolytic cell with a nickel rod as counter electrode. Developing bubbles were periodically removed by re-immersing the foils in the electrolyte.

Large scale patterning could be done with low resolution at the hundreds of micrometer scale by using a permanent marker or with higher resolution down to some $100\ \mu\text{m}$ by printing a pattern directly on the copper foil using a laser printer (with the foil fixed onto a sheet of paper). High resolution patterning using more complex lithography procedures should be possible as well.

Both the ink and the printer toner were removed using acetone and ethanol in an ultrasonic bath after which the substrate cleaning and stretching procedure was repeated. During the following oxidation and expansion, the copper oxide layers usually overlapped the nickel patterns. Different patterns using this procedure are shown in Figure 3.

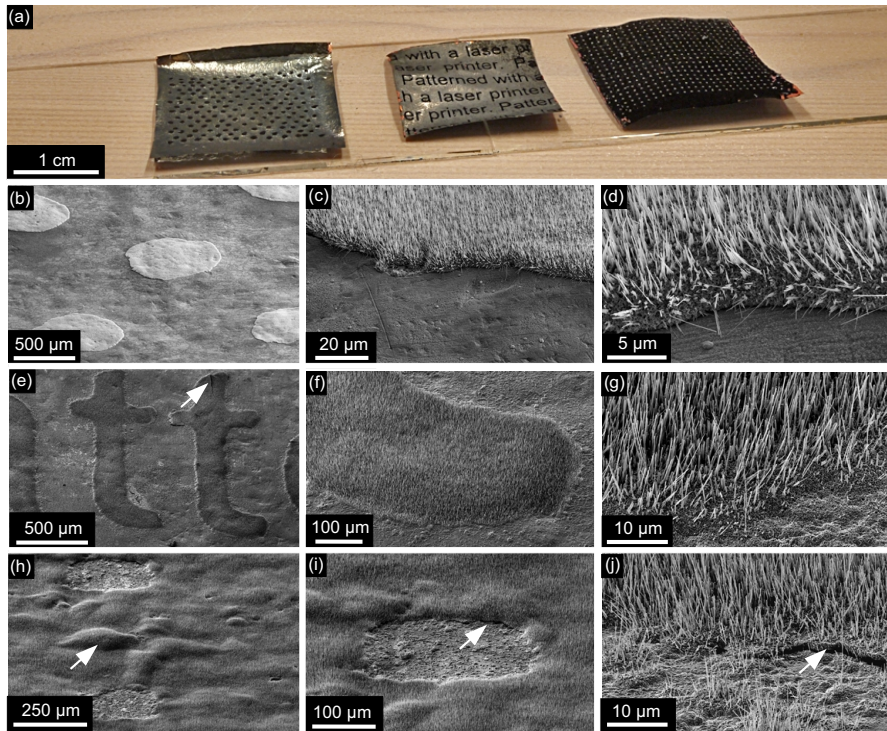


Figure 3. Patterned nanowire growth by Ni deposition: (a): Photo of the samples, (b)-(d): Surface patterned with dots of a permanent marker, (e)-(j): Surfaces patterned with a laser printer. Arrows marking distortions.

From Figure 3, it can be seen that in contrast to flat samples and samples patterned with permanent ink, those patterned with the laser printer show distortions (small bumps and cracks) on their surfaces. Nevertheless, no flaking was observed. The surface modification might be attributed to the heat and pressure present during the printing process. From Figure 3(f) and (j) it is also evident, that some toner was deposited in the supposedly white spots (resulting in nanowire growth in the squares). This often happened, for large black printouts with very small white structures.

3. Discussion and Potential Applications

Comparing the presented approach with the referenced methods, it seems that initial ZnO deposition is beneficial for systems, such as field emission devices, where good electrical contact between the nanowires and the substrate is required, whereas electrodeposition of copper islands and their subsequent oxidation might have

advantages for the integration of CuO nanowire arrays into silicon based technology.

The described method of fabricating large nanowire arrays using flat or structured thin copper foils is on the other hand most suitable for applications, where nanowire arrays are used primarily because of their topography. Such applications already realized with other nanostructures include utilizations as templates[13], as support for catalysts[14], as high roughness building blocks in surface science[15] or as cell guidance[16] or cell transfection[17] units in cell biology. Steps toward two such applications are described in more detail below and illustrated in Figure 4 (see the supplementary material for detailed preparation procedures).

Figure 4(a) to (c) show a sample which was structured into an array of dimples in analogy to Figure 2(a)-(c). Then the dimples were covered with permanent ink as described for Figure 3(b)-(d) and a Ni layer was deposited. Upon oxidation after ink removal, this resulted in selective nanowire growth within the dimples as shown in Figure 4(b).

The sample was used to demonstrate the applicability of the CuO nanowire array as a superhydrophobic surface and the additional benefit obtainable by structuring the substrate. For a superhydrophobic, i.e. highly water repellent surface to form, rough surface features have to be combined with low surface energy. To achieve this, the oxidized sample was incubated in a 1 mM solution of 1H,1H,2H,2H-Perfluorodecanethiol, a layer forming, low surface energy alkanethiol in ethanol. The high surface roughness in the dimples, combined with the fact that alkanethiol solutions form stable layers on CuO[18, 19] but not on NiO[20] resulted in the localized fabrication of a superhydrophobic surface, and hence the trapping of small volumes of air surrounded by water in the dimples. These might e.g. serve as containers for gas phase reactions. Figure 4(a) shows reflections at the interface between the water (coloured with food colour) and the trapped air[21].

Figure 4(d) to (e) show HeLa cells centrifuged onto the nanowire covered CuO surface and subsequently cultured for 4 days. The cells adhered and spread on the surface while being penetrated by the wires. This demonstrates a first step towards using the CuO nanowire array as a delivery tool for biomolecules into cells in analogy to other vertically oriented nanostructures - an area which recently attracts a lot of attention[17, 22, 23, 24].

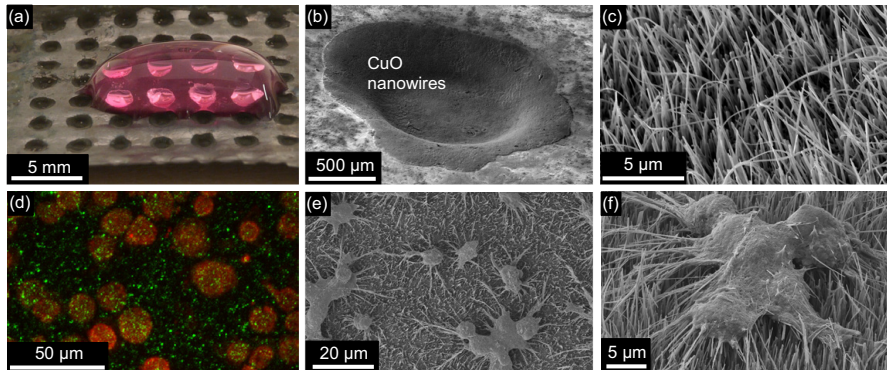


Figure 4. Potential applications:(a)-(c): Surface with superhydrophobic dimples, (a): Water droplet coloured with food colour, light pink areas are reflections at the interface of water and trapped air, black areas are nanowires (b),(c): SEM micrographs. (d)-(f): HeLa cells on nanowires, (d): Fluorescent image of stained cells (red) on photoluminescent nanowires (green), (e),(f): SEM micrographs of fixed cells, top view and detailed side view.

4. Conclusions

We presented a simple method to produce large scale vertically aligned CuO nanowire arrays without any notable flaking on the surface. The whole process from substrate cleaning to using the cooled down, nanowire covered sample takes only about 2.5 hours, is easily implementable and uses solely standard laboratory equipment in combination with comparatively low-cost substrates.

In addition, the substrates could be shaped with millimeter to about 100 μm resolution using a simple pattern transfer mechanism prior to oxidation and nanowire growth could be restricted to defined areas using two electrode nickel electrodeposition.

Substrates covered (and patterned) in that way might be used in applications, where nanowire arrays are employed mostly due to their topography. Two such applications are outlined in the article. As the fabrication procedure is so simple, the presented approach is especially an opportunity for laboratories working in adjacent fields to nanofabrication, such as bionanotechnology or surface science or for student exercises.

Acknowledgments

Acknowledgement The authors thank Kristin G. Sæterbø for assistance with cell culturing. This work was supported by the Nanomat program of the Norwegian research council.

Supporting Material

Detailed descriptions of the correlation between foil thickness and flaking and foil stretching and nanowire density as well as the preparation procedures for superhydrophobic surfaces and cell impaling substrates can be found in the supplementary material.

References

- [1] Jiang X, Herricks T, Xia Y 2002 *Nano Lett.* **2** 1333–1338
- [2] Zhu Y, Yu T, Cheong F, Xu X, Lim C, Tan V, Thong J, Sow C 2005 *Nanotechnology* **16** 88
- [3] Hansen B, Kouklin N, Lu G, Lin I, Chen J, Zhang X 2010 *J Phys. Chem. C* **114** 2440–2447
- [4] Mumm F, van Helvoort A, Sikorski P 2009 *ACS nano* **3** 2647–2652
- [5] Zhou Y, Kamiya S, Minamikawa H, Shimizu T 2007 *Adv. Mater.* **19** 4194 – 4197
- [6] Yu T, Cheong F, Sow C 2004 *Nanotechnology* **15** 1732
- [7] Cheong F C, Grier D G 2010 *Opt. Express* **18** 6555–6562
- [8] Hansen B, Lu G, Chen J 2008 *J. Nanomater.* **2008** 20
- [9] Huang C, Chatterjee A, Liu S, Wu S, Cheng C 2010 *Appl. Surf. Sci.* **256** 3688–3692
- [10] Zhang K, Rossi C, Tenaillon C, Alphonse P, Chane-Ching J 2007 *Nanotechnology* **18** 275607
- [11] Wang R, Li C 2009 *Cryst. Growth Des.* **9** 2229–2234
- [12] Kumar A, Srivastava A, Tiwari P, Nandedkar R 2004 *J. Phys.-Condens. Mat.* **16** 8531–8543
- [13] Kim W, Lee M 2009 *Mater. Lett.* **63** 933–936
- [14] Zhang C, Chen P, Liu J, Zhang Y, Shen W, Xu H, Tang Y 2008 *Chem. Commun.* **2008** 3290–3292
- [15] Lau K, Bico J, Teo K, Chhowalla M, Amaratunga G, Milne W, McKinley G, Gleason K 2003 *Nano Lett.* **3** 1701–1705
- [16] Prinz C, Hällström W, Mårtensson T, Samuelson L, Montelius L, Kanje M 2008 *Nanotechnology* **19** 345101
- [17] Shalek A, Robinson J, Karp E, Lee J, Ahn D, Yoon M, Sutton A, Jorgolli M, Gertner R, Gujral T et al. 2010 *PNAS* **107** 1870
- [18] Sung M, Sung K, Kim C, Lee S, Kim Y 2000 *J. Phys. Chem. B* **104** 2273–2277
- [19] Keller H, Simak P, Schrepp W, Dembowski J 1994 *Thin Solid Films* **244** 799–805
- [20] Mekhalif Z, Riga J, Pireaux J, Delhalle J 1997 *Langmuir* **13** 2285–2290
- [21] Larmour I, Bell S, Saunders G 2007 *Angew. Chem. Int. Ed.* **119** 1740–1742

- [22] Peckys D, Melechko A, Simpson M, McKnight T 2009 *Nanotechnology* **20** 145304
- [23] Park S, Kim Y, Kim W, Jon S 2009 *Nano Lett.* **9** 1325–1329
- [24] Kim W, Ng J, Kunitake M, Conklin B, Yang P 2007 *J. Am. Chem. Soc.* **129** 7228–7229

Oxidative Fabrication of Patterned, Large, Defect-Free CuO Nanowire arrays, Supporting Material

Florian Mumm, Pawel Sikorski

Substrate Thickness and Flaking

1 shows a comparison of a non flaking 25 μm thick copper substrate (99.98 % Cu) with similarly prepared thicker substrates with thicknesses of , 100 μm (99.8 % Cu), 250 μm (99.98 % Cu), and 800 μm (unknown purity) respectively. As seen, only the thinn substrate remains defect free after cooling to room temperature.

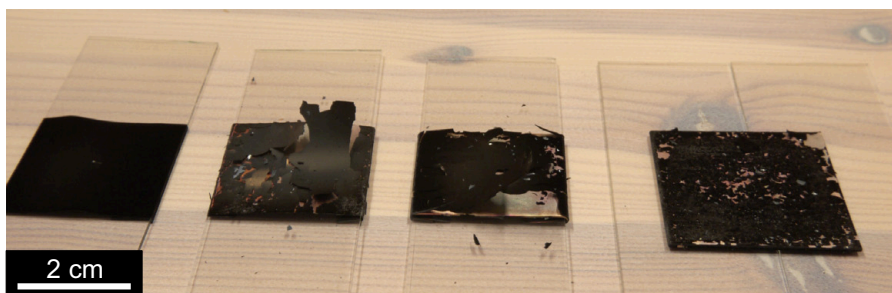


Figure 1: Similarly prepared samples with varying thicknesses, from left: 25 μm , 100 μm , 250 μm , 800 μm

Stretching, Colour, and Nanowire Coverage

Generally, less stretched samples resulted in a coverage with shorter, less dense wires. This could be seen macroscopically by differences in the colour of the samples as shown in 2(a). The figure shows a comparison of a stretched and fixed foil being prepared as outlined at the article and a more relaxed one, which was flattened by rubbing with a rumped wipe and then left on the glass slide without any fixation. Both foils were oxidized at 500 $^{\circ}\text{C}$ for 2 h.

The colour of the foils is a good indication, for its surface coverage. Substrates covered with dense nanowire arrays are dark black. A more greyish appearance indicates a less dense coverage.

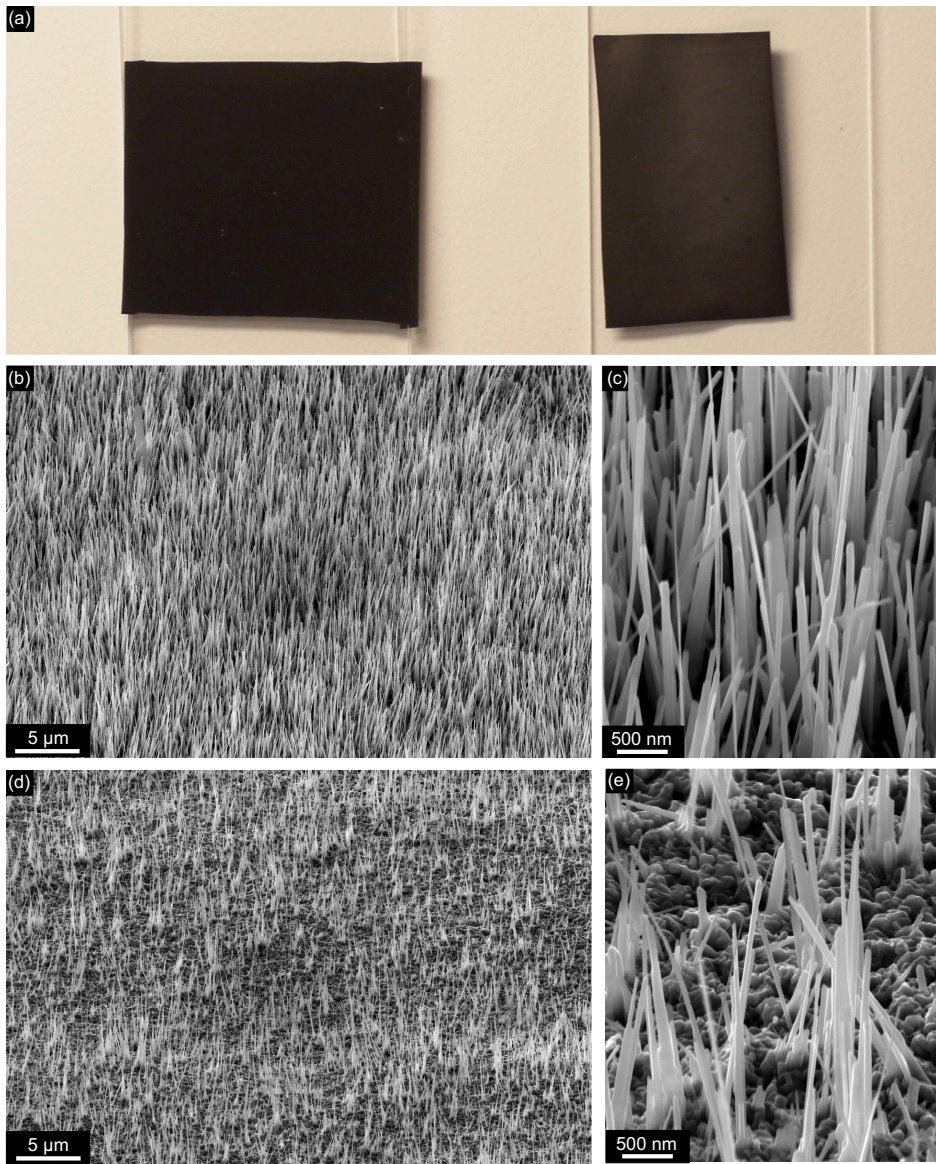


Figure 2: Nanowire covered surface different colours indicating different surface topographies (a): Photograph of foils being oxidized while folded (left) and not folded (right) around a microscope slide, (b),(c): Surface of the folded foil, (d),(e): Surface of the non-folded foil

Preparation of Superhydrophilic dimples

To produce superhydrophobic dimples in a more hydrophilic chip as shown in Figure 4(a) and (b) in the article, mould transfer and selective nanowire growth was combined. First a regular pattern of plastic spikes was used to shape the foil into an array of macroscopic dimples. Then these dimples were covered with water resistant ink from a permanent marker, to exclude them from the subsequent Ni electrodeposition. Deposition was performed as described in the article. Afterwards, the ink was removed with acetone and ethanol and the patterned substrate was cleaned and oxidized.

The result is a sample, where CuO nanowire covered dimples are surrounded by flat parts of NiO. The different surfaces were further functionalized with self assembled layers of alkanethiols. For CuO, this is based on a two step reaction: CuO is first reduced to Cu under disulfide formation followed by binding of unreacted alkanethiols to the newly created copper. Both mono- and multilayers have been reported^{1,2}. In our own experiments, we found an about 30 nm thick multilayer around the CuO nanowires after incubation in a 1 mM solution of 1H,1H,2H,2H-Perfluorodecanethiol (HDFT) in ethanol for 1h³. The same alkanethiol solution was used in this study. Samples were incubated for 45 minutes. In contrast to the assembly on CuO, only poor alkanethiol layers were reported for NiO surfaces⁴.

The used alkanethiol consists of a thiol head group and a tail of low surface energy fluorocarbons. Due to the differences in topography and layer assembly, incubation in HDFT exclusively renders the nanowire part superhydrophobic. When immersed in water, this results in air being trapped in the dimples, as can be seen by the mirror effect visible at the air/ water interface⁵.

Cell Growth on Nanowire Arrays

To impale HeLa cells on the nanowire array, the substrates were sterilized in ethanol and transferred to a sterile bench. 500,000 cells in 1 ml growth medium (Invitrogen DMEM with additions of fetal bovine serum, L - Glutamine and non essential amino acids) were added and subsequently centrifuged onto the wires at 1500g for 5 minutes. The samples were then transferred to 2 ml fresh growth medium and incubated at 37 °C for 4 days.

Prior to confocal imaging and fixation, the cells were stained with Invitrogen CellTracker Red CMTPX. The micrograph in Figure 4(d) in the article is an aggregation of a confocal stack showing the strongest fluorescent intensities for each pixel. This is done to compensate for the sample being not totally flat and parallel to the image planes. After confocal imaging, the samples were fixed in a 2.5% glutaraldehyde solution, dried from ethanol, and sputter coated with platinum to be imaged by scanning electron microscopy. Bending of the wires towards the cells as visible in Figure 4(e) and (f) is probably an artefact of the drying process in the SEM preparation procedure.

References

1. Sung, M.; Sung, K.; Kim, C.; Lee, S.; Kim, Y. *Journal of Physical Chemistry B* **2000**, *104*, 2273–2277
2. Keller, H.; Simak, P.; Schrepp, W.; Dembowski, J. *Thin Solid Films* **1994**, *244*, 799–805
3. Mumm, F.; van Helvoort, A.; Sikorski, P. *ACS nano* **2009**, *3*, 2647–2652
4. Mekhalif, Z.; Riga, J.; Pireaux, J.; Delhalle, J. *Langmuir* **1997**, *13*, 2285–2290
5. Larmour, I.; Bell, S.; Saunders, G. *Angewandte Chemie* **2007**, *119*, 1740–1742

8 Paper III

Is not included due to copyright

Easy Route to Superhydrophobic Copper-Based Wire-Guided Droplet Microfluidic Systems

Supporting Information

Florian Mumm, Antonius T. J. van Helvoort, and Pawel Sikorski

*Department of Physics, Norwegian University of Science and Technology, Høgskoleringen 5,
Trondheim NO-7491, Norway*

E-mail: mumm@phys.ntnu.no; pawel.sikorski@phys.ntnu.no

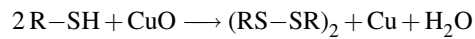
Video

The video in the supplementary material shows a short sequence of the manual operation of the produced digital microfluidic chip. A patterned surface obtained by etching of polycrystalline copper plates was used. As can be seen, the optical fiber is not always inserted in the droplet directly from the top. This might increase the water/fiber contact area and lead to a higher adhesion of the droplet to the fiber than calculated in the main article.

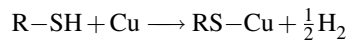
The process in the video shows a repeated cycle of droplet generation, droplet mixing, and fiber cleaning.

Transmission Electron Microscopy Analysis

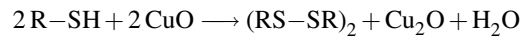
For the analysis of the cupric oxide nanowires incubated in 1H,1H,2H,2H-Perfluorodecanethiol (HDFT) by Transmission Electron Microscopy (TEM) a JEOL 2010F TEM was used. Upon incubation in alkanethiols, CuO is reduced to copper under disulphide formation with subsequent layer deposition according to^{2,3}:



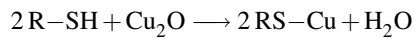
and



or



and



Preparation

For TEM analysis, the nanowires were scraped off the surface on which they were grown with a fresh razor blade and dispersed in ethanol. A droplet of this ethanol solution was then deposited on a 400 mesh copper grid coated with a holey, amorphous carbon film, see Figure 1

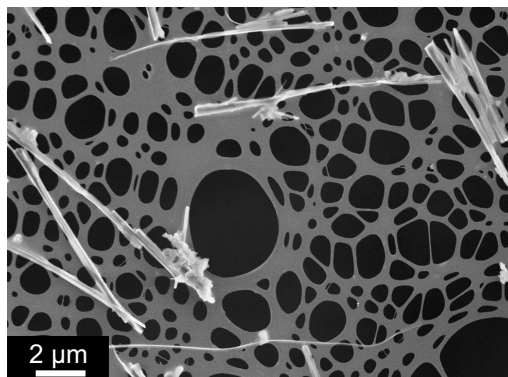


Figure 1: CuO nanowires on the amorphous carbon film

Imaging and Electron Diffraction

Bright field TEM images showed an amorphous coating around a crystalline core structure as seen in Figure 2(a). Using selected area electron diffraction (SAED), the core was discovered to be monoclinic cupric oxide as shown in Figure 2(b).

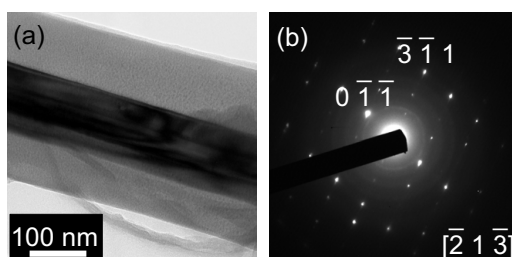


Figure 2: (a): Bright field TEM image of a coated wire, (b): SAED pattern of the core structure of the wire

Electron Energy Loss Spectroscopy

In addition to diffraction, Electron Energy Loss Spectroscopy (EELS) was carried out on the coated nanowires to determine their composition after the incubation in HDFT. The measured spectrum in the energy loss range from 920 to 1000 eV is shown in Figure 3 in comparison to Cu and CuO reference spectra¹. All spectra are background corrected. The measured spectrum has dominating white lines from CuO.

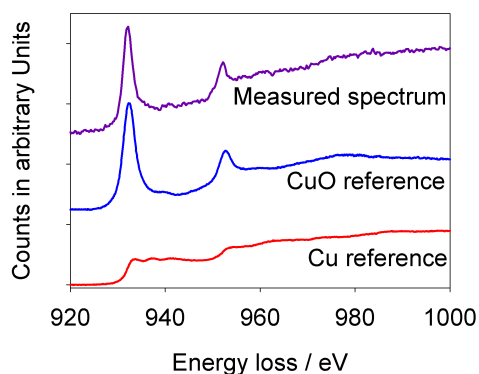


Figure 3: Measured EELS spectrum in comparison with reference values obtained from Ngantcha et al.¹

Energy Dispersive X-ray Spectroscopy

An Energy Dispersive X-ray Spectroscopy (EDS) linescan was obtained to differentiate between the metal and/or metal oxide composed nanowire body and the applied thiol modified fluorocarbon coating. Figure 4 shows the intensity distribution along the wire for copper, oxygen and sulfur, indicating, that the produced structures consist of nanowires surrounded a HDFT coating. The copper signal from the coating, might originate from stray radiation, as a copper grid was used to prepare the TEM sample.

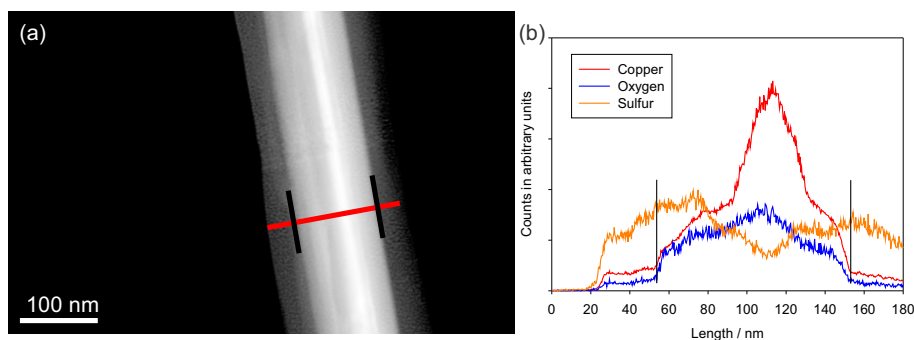


Figure 4: (a): High angle annular dark field STEM image a nanowire. The EDS linescan was done along the red line. (b): Spectrum of elements, the black lines correspond to positions indicated in a. The copper counts are reduced by a factor of 10

Discussion of the TEM Data

Even though the wires change their composition and orientation upon layer formation, a CuO phase is still dominant after the incubation in HDFT. Outer layers might nevertheless be reduced to copper, as described in the main article. During this reaction a fluorocarbon multilayer of several tenth of nm is produced.

This is in agreement with data published by Keller et al.² for multilayer formation of octadecylthiol and propylthiol on oxidized copper surfaces but in contrast to Sung et al.³, who reported monolayer formation in combination with total reduction of a 50 nm layer of CuO on copper upon incubation in hexadecanethiol, octanethiol, and butanethiol.

References

1. Ngantcha, J.; Gerland, M.; Kihn, Y.; Riviere, A. Correlation Between Microstructure and Mechanical Spectroscopy of a Cu-Cu₂O Alloy Between 290 K and 873 K. *Eur. Phys. J-Appl.*

Phys. **2004**, *29*, 83–89

2. Keller, H.; Simak, P.; Schrepp, W.; Dembowski, J. Surface Chemistry of Thiols on Copper: an Efficient Way of Producing Multilayers. *Thin Solid Films* **1994**, *244*, 799–805
3. Sung, M.; Sung, K.; Kim, C.; Lee, S.; Kim, Y. Self-Assembled Monolayers of Alkanethiols on Oxidized Copper Surfaces. *J. Phys. Chem. B* **2000**, *104*, 2273–2277

9 Paper IV

Is not included due to copyright